

Electronic Supplementary Information

Ionic Liquid-Based Compound Droplet Microfluidics for Dynamic ‘On-Drop’ Separations and Sensing

Zahra Barikbin^a, Md. Taifur Rahman^a, Pravien Parthiban^b, Anandkumar S. Rane^a, Vaibhav Jain^a, Suhanya Duraiswamy^b, Su Hui Sophia Lee^a and Saif A. Khan^{*a,b}

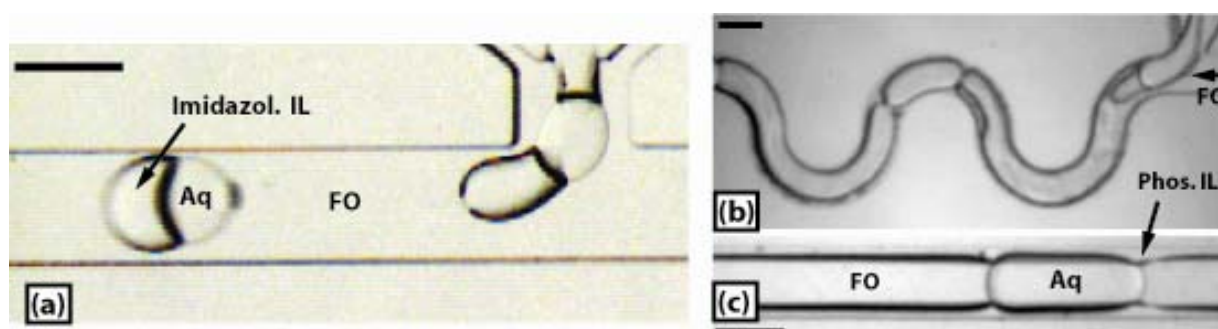


Figure S1. (a) Aqueous- [MMIm][NTf₂] (structure provided in Fig. S2) compound droplet generation in fluorinated oil (b, c) Three-phase flow with phosphonium ionic liquid [C₁₂(C₄)₃P][NTf₂]. Compound droplets are not formed in this case as the ionic liquid does not satisfy a key criterion for compound droplet formation; it competes with the fluorinated oil in wetting the PDMS microchannel surface. Scale bars are 300μm.

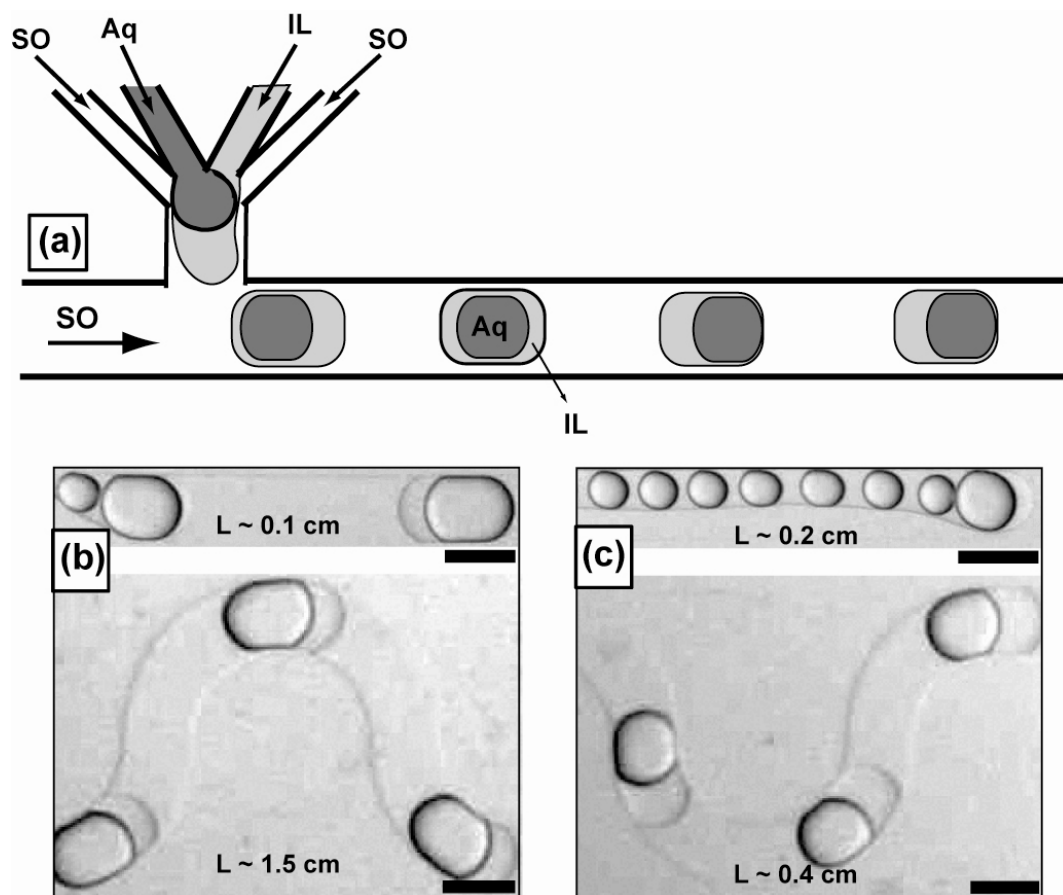
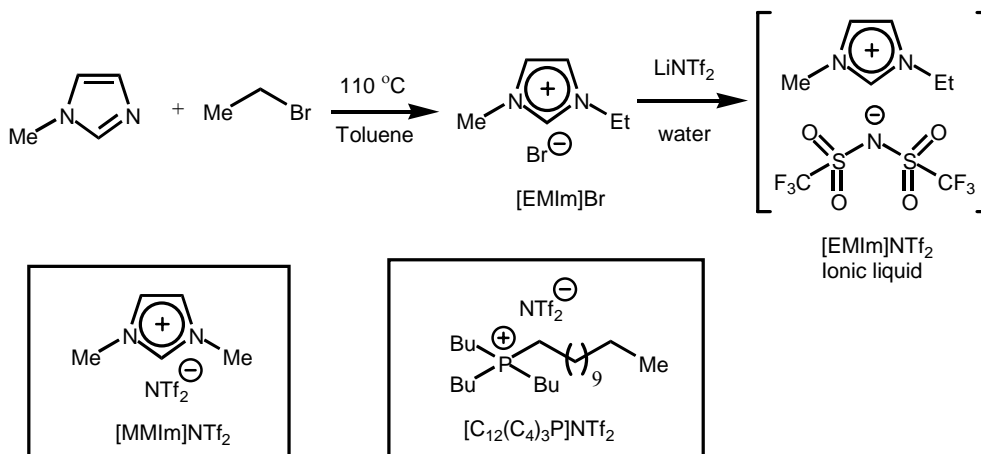
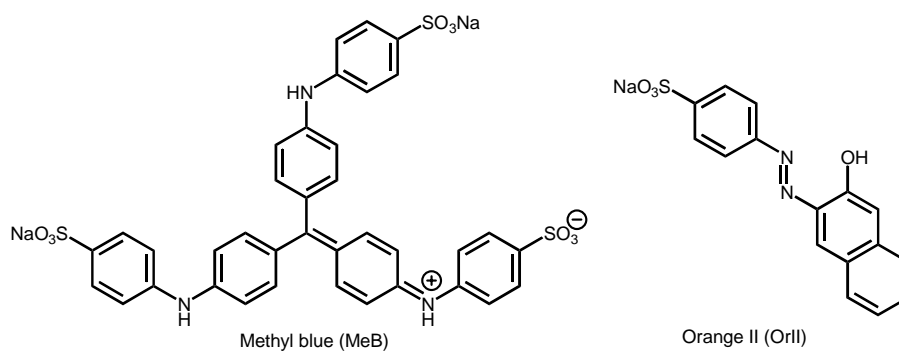


Figure S2. (a) Schematic illustrating the our method and other droplet morphologies obtained with silicone oil as continuous phase (b) - (c) Stereomicroscopic images of different morphologies of the compound droplets obtained with Q_{IL} (b) $2 \mu\text{Lmin}^{-1}$ (c) $5 \mu\text{Lmin}^{-1}$ at constant Q_{Aq} ($5 \mu\text{Lmin}^{-1}$) and Q_{SO} ($15 \mu\text{Lmin}^{-1}$). Scale bars represent $300 \mu\text{m}$.

(a)



(b)



(c)

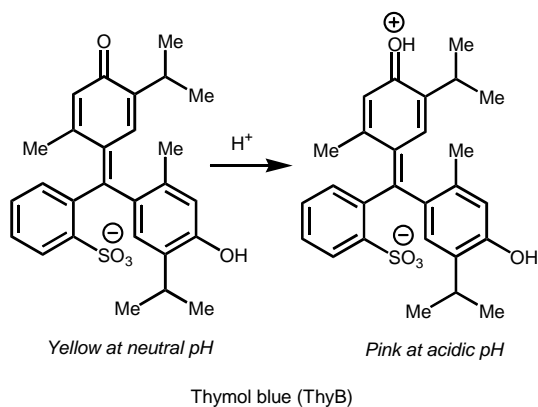


Figure S3. (a) Schematic of [EMIm]NTf₂ Ionic Liquid Synthesis (b) Molecular structures of Orange II and Methyl blue (c) Molecular structures of Thymol blue at different pH

Off-chip batch experiments for measuring pH change in the aqueous phase due to acid mass-transfer into ionic liquid phase containing Thymol Blue indicator:

We operate at aqueous-IL droplet volume ratio 3:1 in our microfluidic pH sensing experiments. Therefore, we conducted batch tests by taking in each case 1 mL of [EMIm]NTf₂ (containing 0.0016 M Thymol blue indicator) solution with 3 mL of aqueous acid solution (para-toluenesulfonic acid monohydrate) of varying acid concentrations in screw-capped glass vials. These biphasic mixtures were vortexed to mix ionic liquid and aqueous phases. Mass transfer of acid from aqueous phase to ionic liquid phase was immediately observed by the intense pink coloration in the latter phase. Then, we measured pH of the aqueous phase (after the partitioning with the IL phase) and compared this with the pH of the original aqueous acid solution (Table ST1).

Table ST1

Aqueous acid concentration	1.0 M	0.50 M	0.10 M	0.05 M	0.01 M	0.005 M
pH* of aqueous acid solution	0.18	0.46	1.07	1.39	2.03	2.35
pH* of aqueous acid solution after partitioning with IL	0.21	0.48	1.10	1.39	2.17	2.58

* Measurement uncertainty ± 0.01

Finite Element Modeling (FEM) of convection-enhanced mass transport in compound droplets using COMSOL Multiphysics 3.5a

We implemented an FEM model of compound droplets in COMSOL Multiphysics 3.5a, where we solved the incompressible Navier-Stokes and time-dependent convection-diffusion equations in coupled fashion as follows:

1. We first solved for the outer (continuous fluid) velocity fields assuming fully mobile inner boundaries. We do this in the frame of reference of the compound droplet, and therefore translate the outer walls at a speed $-U$. We then use the above outer solution as a boundary condition and solve for the inner (aqueous and IL velocity fields). This method of coupling inner and outer solutions is necessarily an approximation, and over-estimates the velocity, especially in the ionic liquid phase. Besides, it does not account for normal stresses due to interfacial tension. However, the advantage is that this scheme is easy to implement, and will not change the essential physics we wish to examine here - a comparison between purely diffusive mass transport and mass transport in the presence of recirculatory convection within a closed compartment.
2. The inner velocity fields were then used as input to the unsteady convection-diffusion equation to calculate time evolution of area-averaged concentration within both aqueous and ionic liquid compartments. We used the following parameters in the simulations: $\mu_{IL} = 30 \times 10^{-3} \text{ Pa.s}$, $\mu_{OIL} = 5.1 \times 10^{-3} \text{ Pa.s}$, $\mu_{H_2O} = 1 \times 10^{-3} \text{ Pa.s}$, $D_{IL} = 6.5 \times 10^{-12} \text{ m}^2 \text{ s}^{-1}$, $D_{H_2O} = 1.69 \times 10^{-10} \text{ m}^2 \text{ s}^{-1}$, $\rho_{OIL} = 1895 \text{ kg m}^{-3}$, $\rho_{H_2O} = 1000 \text{ kg m}^{-3}$, $\rho_{OIL} = 1509 \text{ kg m}^{-3}$. We simulated the system for an aqueous-phase initial concentration $C_{AQ} = 0.75 \text{ mM}$, partition coefficient $K=1$, and a wall speed U of $5.78 \times 10^{-3} \text{ m s}^{-1}$. We ran the simulation for 50 s in time steps of 1 s; the aqueous droplet had an initial concentration of 0.75 mM dye, and the ionic liquid contained no dye at the start of the simulation.

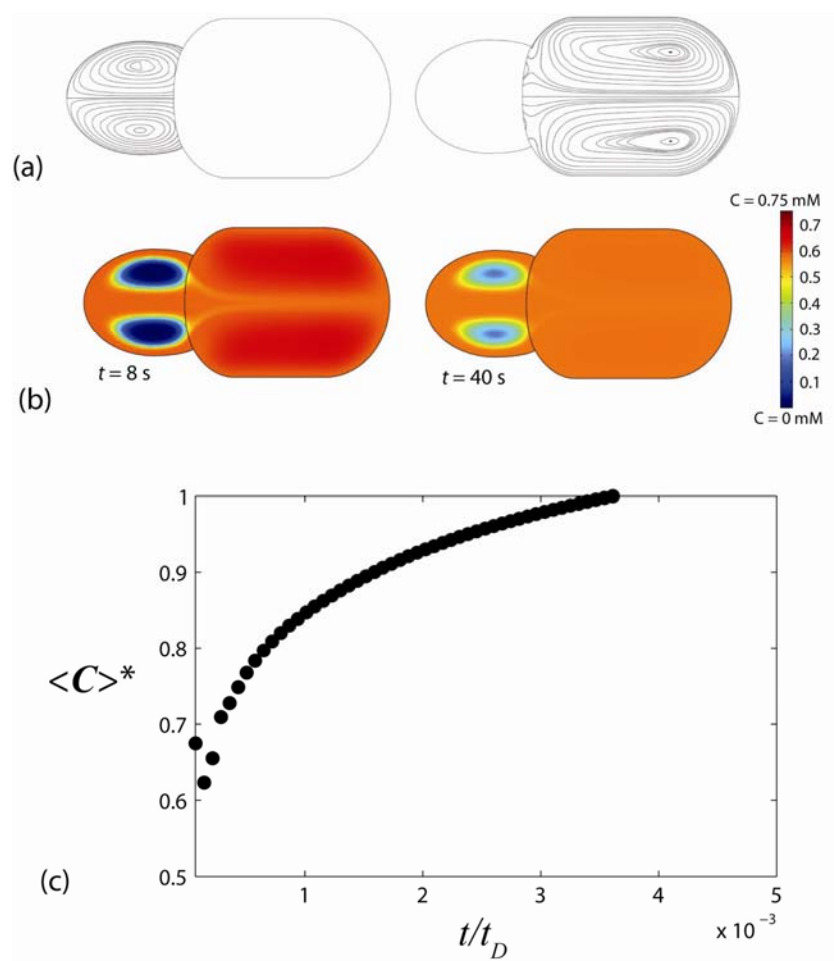


Figure S4. (a) Calculated streamlines in both aqueous and IL compartments, (b) snapshots of concentration in both compartments at two different times, and (c) normalized area averaged concentration ($\langle C \rangle^*$) in ionic liquid compartment as a function of time (normalized with respect to diffusive time $t_D = w^2/D$). The area-averaged concentration is observed to start leveling at normalized times of $\sim 2 \times 10^{-3}$, indicating dramatic acceleration of mass transport by convection (See also Movie M4).